



Dynamic Sliding Mode Control of Nonlinear Systems Using Neural Networks

A. Karami-Mollaei^{1*}, H. Shanechi²

¹Faculty of Electrical and Computer Engineering, Hakim Sabzevari University, Sabzevar, Iran

²Electrical and Computer Engineering Department, Illinois Institute of Technology, Chicago, USA

ABSTRACT: In this paper, dynamic sliding mode control (DSMC) of nonlinear systems using neural networks is proposed. In DSMC, the chattering is removed due to the integrator placed before the input control signal of the plant. However, in DSMC, the augmented system has higher order than the actual system, i.e. the states number of the augmented system is higher than the actual system and then to control of such a system, we must know and identify the new states, or the plant model should be completely known. To solve this problem, we suggest two online neural networks to identify and to obtain a model for the unknown nonlinear system. In the first approach, the neural network training law is based on the available system states and the bound of the observer error is not proved to converge to zero. The advantage of the second training law is only using the system's output and the observer error converges to zero based on the Lyapunov stability theorem. To verify these approaches, Duffing-Holmes chaotic systems (DHC) are used.

Review History:

Received: 22 April 2017

Revised: 28 August 2017

Accepted: 24 October 2017

Available Online: 11 March 2018

Keywords:

Dynamic Sliding Mode Control

Neural Model

Nonlinear System

Duffing-Holmes Chaotic System

1- Introduction

The control of nonlinear systems is still a challenging area in the literature of control systems theory and some efforts have been made to study this subject [1]. However, most of them can only be applied to a certain class of nonlinear systems. For example, feedback linearization is only applicable to a class of nonlinear systems meeting the involutivity condition and can be transformed into the companion form [1]. Many other methods have some limitations. For example, chattering is the most important problem in sliding mode control (SMC) [2]. It has been shown that sliding mode controller (SMC) is a powerful tool in facing uncertainties, disturbances, and noises that always produce difficulties in the realization of the designed controller for real systems [3]. This is due to the invariance property (insensitivity against disturbances), which is stronger than robustness [1-4]. The invariance property motivates researchers to use SMC for various applications [5-8] especially the precise systems [9]. The greatest limitation of SMC is the chattering, i.e. the high (but finite) frequency oscillations with small amplitude, which produces heat losses in electrical power circuits and wear mechanical parts [3, 4]. Four design methodologies have been proposed to overcome this problem: boundary layer, adaptive boundary layer, higher order SMC (HOSMC) and DSMC [2, 3]. Boundary layer and adaptive boundary layer methods cannot preserve the invariance property of SMC [1-3]. HOSMC is proposed to reliably prevent chattering [4, 10]. In higher order SMC, the effect of switching is totally eliminated by moving the switching to the higher order derivatives of desired output [10]. Many algorithms are proposed for implementation of second or higher order SMC [11]. However, the main drawback is that the controller design generally requires the

knowledge of higher-order derivative of plant model [11]. Hitherto, when the relative degree is 2, usually plant model derivative has to be estimated using complicated observer, for example sliding differentiator [12]. In DSMC, an integrator or a low pass filter is placed in front of the system and then time derivative of control input is applied to the augmented system, i.e. system plus the integrator [3] and then chattering is removed. Accordingly, the design of DSMC is challenging because the dimension of the sliding surface is larger than the other approach's since the surface is designed for the augmented system and, then, the plant model should be completely known when one needs to use SMC to control the augmented system [2, 3]. Therefore, in DSMC, the plant model is needed but in HOSMC the derivatives of the plant model must be known. This is the advantage of DSMC to the HOSMC.

In the past decades, neural networks are used as controllers in nonlinear systems [13, 14] and researchers have proposed various neural SMC methods (see [15] and references therein). Generally, these methods can be classified into two categories: direct and indirect approaches [15]. In direct approach, SMC is implemented by a neural network system. But, in indirect approach, neural networks are used to meet a secondary goal to assist controller in SMC. Intelligent approaches such as neural networks can help solve the problem of DSMC to identify the plant model and, then, this is an indirect approach.

The rest of this paper is organized into six sections. The system model and problem formulation are described in section II. In section III, we present the first system identification procedure and corresponding DSMC. In section IV, the second model identification and a corresponding DSMC are presented. Finally, in section V, we discuss simulation and comparison results to verify theoretical concepts presented in previous sections. The conclusion is given in section VI.

Corresponding author; Email: karami@hsu.ac.ir

2- Problem Formulation

Consider the following single input nonlinear system:

$$\begin{aligned} \dot{x}_i &= x_{i+1} \quad i=1,2,\dots,n-1, \\ \dot{x}_n &= f(x)+u, \\ y &= C^T x, \end{aligned} \quad (1)$$

where $x=[x_1,x_2,\dots,x_n]^T$ is a vector state, u is the input control signal and y is the system output dependent to the states via vector $C \in R^{n \times 1}$ and, moreover, the function $f(x)$ is unknown. The other form of this equation is as follows:

$$\begin{aligned} \dot{x} &= Ax + Bu + Bg(x), y = C^T x, \\ g(x) &= f(x) + \sum_{i=1}^n a_i x_i, \end{aligned} \quad (2)$$

and

$$A = \begin{bmatrix} 0 & 1 & 0 & \dots & 0 \\ 0 & 0 & 1 & \ddots & \vdots \\ \vdots & \vdots & \ddots & \ddots & 0 \\ 0 & 0 & \dots & 0 & 1 \\ -a_1 & -a_2 & \dots & -a_{n-1} & -a_n \end{bmatrix}, B = \begin{bmatrix} 0 \\ 0 \\ \vdots \\ 0 \\ 1 \end{bmatrix}. \quad (3)$$

Assume that $a_i, i=1,2,\dots,n$ are such that A is a Hurwitz matrix i.e. for a symmetric positive definite matrix Q , there exists a symmetric positive definite matrix P satisfying the following Lyapunov equation:

$$A^T P + PA = -Q \quad (4)$$

Our purpose is using DSMC to find a suitable smooth u such that, $x=[x_1,x_2,x_3,\dots,x_n]^T$ and augmented state $x_{n+1}=\dot{x}_n$ converge to zero. Due to the use of DSMC, closed-loop system is invariant and has acceptable performance. Note that invariance is the inherent property of sliding mode control (SMC) and is stronger than robustness. In DSMC, the switching is filtered due to the integrator which is placed before the input control of the system; then chattering is removed and we will have a smooth u . To this aim, an appropriate sliding surface is defined as follows:

$$s = \lambda x + \lambda_{n+1} x_{n+1}, \lambda = [\lambda_1, \lambda_2, \lambda_3, \dots, \lambda_n] \quad (5)$$

Moreover, note that $x=[x_1,x_2,x_3,\dots,x_n]^T$ and x_{n+1} converge to zero if s becomes zero and the coefficients $\lambda_1, \lambda_2, \dots, \lambda_{n+1}$ are properly chosen such that the polynomial $\lambda_{n+1} S^n + \lambda_n S^{n-1} + \dots + \lambda_2 S + \lambda_1 = 0$ is Hurwitz. However, there is a problem with calculation of this surface. The variable x_{n+1} cannot be evaluated due to the unknown function $f(x)$. To solve this problem, neural observers are constructed.

Based on the literature, the neural networks can approximate any real continuous function with an arbitrary accuracy [3, 13]. This means that these networks have universal approximation property [3, 13]. Accordingly, there exists an ideal but unknown weight vector $w \in R^m$ with an arbitrary large enough dimension m such that the system can be written as follows:

$$\begin{aligned} \dot{x} &= Ax + Bu + Bg, y = C^T x \\ g &= w^T \xi(x) + \varepsilon_x \end{aligned} \quad (6)$$

In which ε_x is an arbitrary small reconstruction error with bound B_ε , i.e. $|\varepsilon_x| < B_\varepsilon$ and moreover, $\xi(x): R^n \rightarrow R^m$ is the transfer function of the hidden neurons. Now, we propose two procedures to construct neural observers.

3- First Proposed Approach

3- 1- Model Identification

Now, an estimate of (6) is given by:

$$\begin{aligned} \dot{\hat{x}} &= A\hat{x} + Bu + B\hat{g} \\ \hat{g}(x) &= \hat{w}^T \xi(\hat{x}) \\ \hat{y} &= C^T \hat{x} \end{aligned} \quad (7)$$

Defining the observer error as $\tilde{x} = x - \hat{x}$ and weight vector error as $\tilde{w} = w - \hat{w}$ and $\tilde{\xi}(x) = \xi - \hat{\xi}$ where $\xi = \xi(x)$ and $\hat{\xi} = \xi(\hat{x})$ and using (6) and (7), the error dynamics can be expressed as:

$$\begin{aligned} \dot{\tilde{x}}(t) &= A\tilde{x} + B(w^T \xi - \hat{w}^T \hat{\xi} + \varepsilon_x) \\ &= A\tilde{x} + B(w^T \xi - \hat{w}^T \hat{\xi} - w^T \hat{\xi} + w^T \hat{\xi} + \varepsilon_x) \\ &= A\tilde{x} + B(w^T \tilde{\xi} + \tilde{w}^T \hat{\xi} + \varepsilon_x) \end{aligned} \quad (8)$$

Theorem 1: The observer error $\tilde{x} = x - \hat{x}$ in (8) converges to the inside of the bound $B_{\tilde{x}}$ if the weights are updated according to the following equation:

$$\dot{\hat{w}} = -\eta \hat{\xi}^T \tilde{x}^T A^{-1} B - \rho \|\tilde{x}\| \hat{w}, \quad (9)$$

$$B_{\tilde{x}} = \frac{\|P\| (4B_w B_\xi + B_\varepsilon) + 2B_\xi B_w \|E\| + 6B_w^2}{0.5\sigma(Q)}, \quad (10)$$

where $\|w\| \leq B_w, \|\hat{w}\| \leq B_w, E = \eta \rho^{-1} A^{-1}, \eta > 0$ is the learning rate and ρ is a small positive number.

Proof: Consider a Lyapunov function candidate as follows:

$$V = \frac{1}{2} \tilde{x}^T P \tilde{x} + \frac{1}{2} \tilde{w}^T \rho^{-1} \tilde{w}, \quad (11)$$

where $P = P^T > 0$ and the time derivative of (11) is given by:

$$\dot{V} = \frac{1}{2} \tilde{x}^T P \dot{\tilde{x}} + \frac{1}{2} \tilde{x}^T P \dot{\tilde{x}} + \tilde{w}^T \rho^{-1} \dot{\tilde{w}} \quad (12)$$

By inserting (8), (9), and (4) into (12) and using the equality $\tilde{w} = -\dot{\hat{w}}$ one obtains:

$$\begin{aligned} \dot{V} &= -\frac{1}{2} \tilde{x}^T Q \tilde{x} + \tilde{x}^T P B (w^T \tilde{\xi} + \tilde{w}^T \hat{\xi} + \varepsilon_x) \\ &\quad + \tilde{w}^T \hat{\xi}^T \tilde{x}^T E B + \tilde{w}^T \|\tilde{x}\| (w - \tilde{w}). \end{aligned} \quad (13)$$

Then:

$$\begin{aligned} \tilde{w}^T (w - \tilde{w}) &\leq B_w \|\tilde{w}\| - \|\tilde{w}\|^2 \\ &\leq 2B_w^2 + 4B_w^2 = 6B_w^2, \end{aligned} \quad (14)$$

$$\tilde{w}^T \hat{\xi}^T \tilde{x}^T E B \leq B_\xi \|\tilde{w}\| \|\tilde{x}\| \|E\| \leq 2B_w B_\xi \|E\| \|\tilde{x}\|.$$

such that $\|\tilde{w}\| \leq 2B_w, \|\xi\| \leq B_\xi, \|\hat{\xi}\| \leq B_\xi$ and $\|\tilde{\xi}(x)\| \leq 2B_\xi$. Now using (13) and (14) results in:

$$\begin{aligned} \dot{V} &\leq -\frac{1}{2} \sigma(Q) \|\tilde{x}\|^2 + \|\tilde{x}\| \|P\| (4B_w B_\xi + B_\varepsilon) \\ &\quad + 2B_\xi B_w \|E\| \|\tilde{x}\| + (2B_w^2 + 4B_w^2) \|\tilde{x}\|, \end{aligned} \quad (15)$$

where σ denotes minimum singular value. Furthermore, by using bound (10), we obtain the following equation:

$$\dot{V}(t) \leq -0.5\sigma(Q) (\|\tilde{x}\| - B_{\tilde{x}}) \|\tilde{x}\| \quad (16)$$

Assume that $\omega(t) = 0.5\sigma(Q) (\|\tilde{x}\| - B_{\tilde{x}}) \|\tilde{x}\|$ and $\|\tilde{x}\| > B_{\tilde{x}}$. Then,

one can say that $\dot{V} \leq -\omega(t) \leq 0$. Integrating from zero to t yields:

$$0 \leq \int_0^t \omega(\tau) d\tau \leq \int_0^t \omega(\tau) d\tau + V(t) \leq V(0) \quad (17)$$

when $t \rightarrow \infty$, the above integral exists and is less than or equal to $V(0)$. Since $V(0)$ is positive and finite, according to the Barbalat's lemma [1], we will have:

$$\lim_{t \rightarrow \infty} \omega(t) = \lim_{t \rightarrow \infty} 0.5\sigma(Q) (\|\tilde{x}\| - B_{\tilde{x}}) \|\tilde{x}\| = 0 \quad (18)$$

Since $0.5\sigma(Q)$ is greater than zero, (18) implies that $\|\tilde{x}\|$ decreases until it becomes less than $B_{\tilde{x}}$, i.e.

$$\lim_{t \rightarrow \infty} \|\tilde{x}\| \leq B_{\tilde{x}}.$$

This guarantees that $B_{\tilde{x}}$ is the upper bound of $\|\tilde{x}\|$.

Remark 1: As mentioned in the introduction, this approach has two disadvantages. Firstly, we assume that the system's states are accessible and, secondly, only boundedness of the observer error to bound $B_{\tilde{x}}$ is guaranteed. However, this bound may be large. These two issues will be solved in the second proposed approach.

3- 2- Design of DSMC

From equations (5) and (7), we have:

$$\begin{aligned} s &= \lambda x + \lambda_{n+1} (FA\hat{x} + FBu + FB\hat{g}) \\ &= \lambda x + \lambda_{n+1} (FA\hat{x} + u + \hat{g}), \end{aligned} \quad (19)$$

where $F = [0, 0, \dots, 0, 1] \in R^{1 \times n}$ and therefore:

$$\begin{aligned} \dot{s} &= \lambda \dot{x} + \lambda_{n+1} (FA\dot{\hat{x}} + \dot{u} + \dot{\hat{g}}) \\ &= \sum_{i=1}^{n-1} \lambda_i \dot{\hat{x}}_{i+1} + \lambda_n (FA\dot{\hat{x}} + u + \dot{\hat{g}}) \\ &+ \lambda_{n+1} (FA(A\dot{\hat{x}} + Bu + B\dot{\hat{g}}) + \dot{u} + F\dot{\hat{g}}) \\ &= \sum_{i=1}^{n-1} \lambda_i \dot{\hat{x}}_{i+1} + \lambda_n (FA\dot{\hat{x}} + u + \hat{w}^T \dot{\xi}) \\ &+ \lambda_{n+1} (FA^2 \dot{\hat{x}} + FABu + FAB\dot{\hat{g}} + \dot{u} + \dot{\hat{g}}) \end{aligned} \quad (20)$$

Such that $\dot{\hat{g}}$ is known and can be calculated from equations (7) and (9) as follows:

$$\begin{aligned} \dot{\hat{g}}(x) &= \hat{w}^T \dot{\xi} + \hat{w}^T \dot{\xi} \\ &= (-\eta \hat{\xi}^T A^{-1} B - \rho \|\tilde{x}\| \hat{w})^T \dot{\xi} + \hat{w}^T \frac{\partial \xi(\hat{x})}{\partial \hat{x}} \dot{\hat{x}} \\ &= (-\eta \hat{\xi}^T A^{-1} B - \rho \|\tilde{x}\| \hat{w})^T \dot{\xi} \\ &+ \hat{w}^T \frac{\partial \xi(\hat{x})}{\partial \hat{x}} (A\hat{x} + Bu + B\hat{w}^T \xi). \end{aligned} \quad (21)$$

Theorem 2: The following dynamical equation causes the sliding surface s as in (19) converges to zero:

$$\begin{aligned} \dot{u} &= \frac{-k_1 \text{sign}(s) - k_2 s - \sum_{i=1}^{n-1} \lambda_i \dot{\hat{x}}_{i+1}}{\lambda_{n+1}} \\ &+ \frac{-\lambda_n (FA\hat{x} + u + \hat{w}^T \xi)}{\lambda_{n+1}} \\ &- (FA^2 \hat{x} + FABu + FAB\hat{g} + \dot{\hat{g}}), \end{aligned} \quad (22)$$

$$k_1 > 0 \text{ and } k_2 > 0 \quad (23)$$

Proof: Consider the Lyapunov function $V = 0.5s^2$, then, $\dot{V} = s\dot{s}$ and replacing \dot{u} from equation (22) into (20) follows that:

$$\dot{s} = -k_1 \text{sign}(s) - k_2 s \quad (24)$$

Hence:

$$\dot{V} = -k_1 |s| - k_2 s^2 \leq -k_1 |s| \quad (25)$$

Suppose t_f is the finite reaching time to the sliding surface, i.e. $s(t_f) = 0$, then, it is easy to show that $t_f \leq |s(0)|/k_1$.

4- Second Proposed Approach

4- 1- Model Identification

In the second approach, the proposed observer for (6) is given by:

$$\begin{aligned} \dot{\hat{x}} &= A\hat{x} + B(u + \hat{g} + k_x(y - \hat{y})) + T(y - \hat{y}) \\ \hat{g}(x) &= \hat{w}^T \xi(\hat{x}) = \hat{w}^T \hat{\xi} \end{aligned} \quad (26)$$

where observer gain vector $T \in R^{n \times 1}$ are chosen such that $A_s = A - TC^T$ is stable, i.e., for any symmetric positive definite matrix Q , there exists a symmetric positive definite matrix P satisfying the following Lyapunov equation,

$$A_s^T P + P A_s = -Q. \quad (27)$$

By subtracting (26) from (6), we obtain:

$$\begin{aligned} \dot{\tilde{x}} &= A\tilde{x} + B(w^T \xi(x) + \varepsilon_x) \\ &- B(\hat{w}^T \xi(\hat{x}) + k_x(y - \hat{y})) - T(y - \hat{y}) \\ &= A_s \tilde{x} + B(w^T \xi(x) - \hat{w}^T \xi(\hat{x})) \\ &+ B(-k_x(y - \hat{y}) + \varepsilon_x) \\ &+ B(w^T \xi(x) - \hat{w}^T \xi(\hat{x}) - k_x(y - \hat{y}) + \varepsilon_x) \\ &= A_s \tilde{x} + B(w^T \xi(x) - \hat{w}^T \xi(\hat{x}) - w^T \xi(\hat{x})) \\ &+ B(w^T \xi(\hat{x}) - k_x(y - \hat{y}) + \varepsilon_x) \\ &= A_s \tilde{x} + B(\tilde{w}^T \xi + w^T \tilde{\xi} - k_x(y - \hat{y}) + \varepsilon_x). \end{aligned} \quad (28)$$

Theorem 3: By using the following adaptive weight law:

$$\dot{\hat{w}} = k_w \hat{\xi} \tilde{y} - 4k_e k_w |\tilde{y}| \hat{w} \quad (29)$$

the estimation error $\tilde{x}(t)$ converges to zero if $k_x \rightarrow \infty$ with $k_w > 0$ and $k_e > 0$ and $\tilde{y} = y - \hat{y}$.

Proof: Consider the following Lyapunov function:

$$V(t) = \frac{1}{2} \tilde{x}^T P \tilde{x} + \frac{1}{2k_w} \tilde{w}^T \tilde{w} \quad (30)$$

Taking the derivative of $V(t)$ with respect to time yields:

$$\dot{V}(t) = \frac{1}{2} \dot{\tilde{x}}^T P \tilde{x} + \frac{1}{2} \tilde{x}^T P \dot{\tilde{x}} + \frac{1}{k_w} \tilde{w}^T \dot{\tilde{w}} \quad (31)$$

Inserting (27) and (28) into the above equation indicates that :

$$\begin{aligned} \dot{V}(t) &= -\frac{1}{2} \tilde{x}^T Q \tilde{x} + \tilde{x}^T P B (w^T \xi + \varepsilon_x) \\ &- k_x \tilde{x}^T C B^T P \tilde{x} + \tilde{w}^T \left(\frac{1}{k_w} \dot{\tilde{w}} + \hat{\xi} B^T P \tilde{x} \right) \end{aligned} \quad (32)$$

Using the equality $\dot{\tilde{w}} = -\dot{\hat{w}}$ and tuning law (29) in the above equation leads to:

$$\begin{aligned} \dot{V}(t) = & -\frac{1}{2} \tilde{x}^T Q \tilde{x} + \tilde{x}^T P B (w^T \tilde{\xi} + \varepsilon_x) \\ & - k_x \tilde{x}^T C B^T P \tilde{x} + 4k_e |\tilde{y}| \tilde{w}^T \hat{w}. \end{aligned} \quad (33)$$

Here, consider the properties of positive definite matrices Q and P , and using $\hat{w} = w - \tilde{w}$, the above equation yields:

$$\begin{aligned} \dot{V}(t) \leq & -\left(0.5\sigma(Q) + k_x \sigma(CB^T P)\right) \|\tilde{x}\|^2 \\ & + \bar{\sigma}(PB)(2B_w B_\xi + B_e) \|\tilde{x}\| \\ & - 4k_e (\|\tilde{w}\|^2 - B_w \|\tilde{w}\|) |\tilde{y}|. \end{aligned} \quad (34)$$

whereas $|w^T \tilde{\xi} + \varepsilon_x| \leq 2B_w B_\xi + B_e$. Now, we define $B_{\tilde{x}}$ as follows:

$$B_{\tilde{x}} = \frac{\bar{\sigma}(PB)(2B_w B_\xi + B_e) + k_e B_w^2 \|C\|}{0.5\sigma(Q) + k_x \sigma(CB^T P)}, \quad (35)$$

where $\bar{\sigma}$ and σ denote maximum and minimum singular values, respectively; therefore:

$$\dot{V}(t) \leq -\left(0.5\sigma(Q) + k_x \sigma(CB^T P)\right) \quad (36)$$

$$\left(\|\tilde{x}\| - B_{\tilde{x}}\right) \|\tilde{x}\| - 4k_e \left(\|\tilde{w}\| - \frac{1}{2} B_w\right)^2 |\tilde{y}|,$$

or:

$$\begin{aligned} \dot{V}(t) \leq & -\left(0.5\sigma(Q) + k_x \sigma(CB^T P)\right) \\ & \left(\|\tilde{x}\| - B_{\tilde{x}}\right) \|\tilde{x}\|. \end{aligned} \quad (37)$$

Take $\omega(t) = \left(0.5\sigma(Q) + k_x \sigma(CB^T P)\right) \left(\|\tilde{x}\| - B_{\tilde{x}}\right) \|\tilde{x}\|$ and suppose $\|\tilde{x}\| > B_{\tilde{x}}$; then, one can write $\dot{V} \leq -\omega(t) \leq 0$. Integrating \dot{V} from 0 into t yields:

$$0 \leq \int_0^t \omega(\tau) d\tau \leq \int_0^t \omega(\tau) d\tau + V(t) \leq V(0). \quad (38)$$

when $t \rightarrow \infty$, the above integral exists and is less than or equal to $V(0)$. Since $V(0)$ is positive and finite, according to the Barbalat's lemma [1], we will have:

$$\begin{aligned} \lim_{t \rightarrow \infty} \omega(t) = \\ \lim_{t \rightarrow \infty} \left(0.5\sigma(Q) + k_x \sigma(CB^T P)\right) \left(\|\tilde{x}\| - B_{\tilde{x}}\right) \|\tilde{x}\| = 0 \end{aligned} \quad (39)$$

Since $\left(0.5\sigma(Q) + k_x \sigma(CB^T P)\right)$ is greater than 0, (39) implies that $\|\tilde{x}\|$ decreases until it becomes less than $B_{\tilde{x}}$ whose result is

$$\lim_{t \rightarrow \infty} \|\tilde{x}\| \leq B_{\tilde{x}}.$$

This guarantees that $B_{\tilde{x}}$ is the upper bound of $\|\tilde{x}\|$ and it is clear that $\lim_{k_x \rightarrow \infty} B_{\tilde{x}} = 0$.

Then, $\|\tilde{x}\|$ or \tilde{x} will converge to zero if $k_x \rightarrow \infty$.

4- 2- Design of DSMC

From equations (5) and (26), we have:

$$\begin{aligned} s = \lambda x \\ + \lambda_{n+1} (FA\hat{x} + u + \hat{g} + k_x(y - \hat{y}) + FT(y - \hat{y})). \end{aligned} \quad (40)$$

Therefore:

$$\begin{aligned} \dot{s} = & \lambda \dot{x} + \lambda_{n+1} (FA\dot{\hat{x}} + \dot{u} + \dot{\hat{g}}) \\ & + \lambda_{n+1} (k_x(\dot{y} - \dot{\hat{y}}) + FT(\dot{y} - \dot{\hat{y}})) \\ = & \sum_{i=1}^{n-1} \lambda_i \dot{\hat{x}}_{i+1} + \lambda_n (FA\dot{\hat{x}} + u + \hat{g}) \\ & + \lambda_n (k_x(y - \hat{y}) + FT(y - \hat{y})) \\ + & \lambda_{n+1} \left([FA - k_x C^T - FTC^T] [A\hat{x} + Bu + B\hat{g}] \right) \\ & + \lambda_{n+1} \left([FA - k_x C^T - FTC^T] [k_x B(y - \hat{y})] \right) \\ & + \lambda_{n+1} \left([FA - k_x C^T - FTC^T] [T(y - \hat{y})] \right) \\ & + \lambda_{n+1} (\dot{u} + \dot{\hat{g}} + \phi), \\ \phi = & k_x \dot{y} + FT\dot{y} = k_x C^T \dot{x} + FTC^T \dot{x} \\ = & (k_x C^T + FTC^T) \dot{x}. \end{aligned} \quad (41)$$

Such that $\dot{\hat{g}}$ is known and can be calculated from equations (26) and (29) as follows:

$$\begin{aligned} \dot{\hat{g}}(x) = & \hat{w}^T \dot{\xi} + \hat{w}^T \dot{\xi} = (k_w \xi^T \tilde{y} - 4k_e k_w |\tilde{y}| \hat{w})^T \dot{\xi} \\ & + \hat{w}^T \frac{\partial \xi(\hat{x})}{\partial \hat{x}} \dot{\hat{x}} = (k_w \xi^T \tilde{y} - 4k_e k_w |\tilde{y}| \hat{w})^T \dot{\xi} \\ & + \hat{w}^T \frac{\partial \xi(\hat{x})}{\partial \hat{x}} (A\hat{x} + Bu + B\hat{w}^T \xi) \\ & + \hat{w}^T \frac{\partial \xi(\hat{x})}{\partial \hat{x}} (k_x B(y - \hat{y}) + T(y - \hat{y})). \end{aligned} \quad (42)$$

Moreover, the unknown terms are placed in ϕ . Variable ϕ is considered as uncertainty due to its dependency to the unknown variable $\dot{y} = C^T \dot{x}$.

Theorem 4: The following dynamical equation causes the sliding surface s as in (40) to converge to zero:

$$\begin{aligned} \dot{u} = & \frac{-k_1 \text{sign}(s) - k_2 s - \sum_{i=1}^{n-1} \lambda_i \dot{\hat{x}}_{i+1}}{\lambda_{n+1}} \\ & - \frac{\lambda_n (FA\hat{x} + u + \hat{g} + k_x(y - \hat{y}) + FT(y - \hat{y}))}{\lambda_{n+1}} \end{aligned} \quad (43)$$

$$\begin{aligned} - & \left([FA - k_x C^T - FTC^T] [A\hat{x} + Bu + B\hat{g}] \right) \\ - & \left([FA - k_x C^T - FTC^T] [k_x B(y - \hat{y})] \right) \\ - & \left([FA - k_x C^T - FTC^T] [T(y - \hat{y})] + \dot{\hat{g}} \right), \end{aligned}$$

$$k_1 = \lambda_{n+1} B_\phi + \varepsilon, \quad \varepsilon > 0 \quad \text{and} \quad k_2 > 0. \quad (44)$$

where B_ϕ is the bound of ϕ , i.e. $|\phi| \leq B_\phi$.

Proof: Consider the Lyapunov function $V = 0.5s^2$, then, $\dot{V} = s\dot{s}$ and, moreover, replacing \dot{u} from (43) into (41) follows that:

$$\dot{s} = -k_1 \text{sign}(s) - k_2 s + \lambda_{n+1} \phi \quad (45)$$

Hence:

$$\begin{aligned} \dot{V} &= -k_1 |s| - k_2 s^2 + \lambda_{n+1} \phi s \\ &\leq -(k_1 - \lambda_{n+1} \phi) |s| \leq -(k_1 - \lambda_{n+1} B_\phi) |s|. \end{aligned} \quad (46)$$

Now, consider k_1 as in (44). Then:

$$\dot{V} \leq -\varepsilon |s|. \quad (47)$$

Suppose t_f is the finite reaching time to the sliding surface, i.e. $s(t_f) = 0$, then, it is easy to show that $t_f \leq |s(0)| / \varepsilon$.

5- Simulation Result

In the following examples, the proposed method is applied to a nonlinear system to show the effectiveness of these approaches. Consider the following model of Duffing-Holmes chaotic systems (DHC) [16, 17]:

$$\begin{aligned} \dot{x}_1 &= x_2 \\ \dot{x}_2 &= f(x, u) \\ &= b_1 x_1 + b_2 x_2 + b_3 x_1^3 + b_4 \cos(1.2t) + u \end{aligned} \quad (48)$$

$$x = [x_1, x_2]^T$$

where b_2 is the damping ratio, $b_1 x_1 + b_3 x_1^3$ is the recoverability term, $b_4 \cos(1.2t)$ is the force period term and u is the input control signal [16]. We select $b_1 = 1$, $b_2 = -0.2$, $b_3 = -1$, $b_4 = 0.32$ and $x(0) = [-2, 1]^T$ where (48) is in the chaotic case which is shown in figure 1. Moreover, $\hat{x}(0) = [0, 0]^T$ and also $\lambda = [10, 10]$, $\lambda_3 = 0.1$. The initial conditions of the weight vector are all set to zero and:

$$A = \begin{bmatrix} 0 & 1 \\ -2 & -4 \end{bmatrix}, w = \begin{bmatrix} 0 & 0 & 0 \\ 0 & 0 & 0 \end{bmatrix} \quad (49)$$

and also:

$$\begin{aligned} \xi_1 &= 2 / (1 + \exp(-2[1, 0]x)) - 1 \\ \xi_2 &= 2 / (1 + \exp(-2[0, 1]x)) - 1 \end{aligned} \quad (50)$$

The simulations are done by MATLAB with the sample time 0.01. The controller parameters are chosen as $k_1 = 0.17$ and $k_2 = 20$.

Example 1: In this example, the first proposed approach in section 3 has been simulated. The network tuning parameters are chosen as $\eta = 50$ and $\rho = 10$. Figures 2, 3, 4 and 5 show the simulation results. From Figure 3, we can see the stability of the closed-loop system and neural observer since the system states converge to zero. Figure 4.a shows the input control signal which is without chattering. Note that Figure 4.b is not important for us because it is before the integrator and is not applied to the system.

Example 2: In this example, the second proposed approach in section 4 has been simulated. The network tuning parameters are chosen as $k_w = 5$, $k_e = 3$ and $k_x = 50$ and also $C = [0, 1]^T$. Figures 6, 7, 8 and 9 show the simulation results.

Comparison: We can see the convergence in example 2 is better because the bound $B_{\bar{x}}$ converges to zero in example 2.

6- Conclusion

In this paper, two new approaches for the control of nonlinear systems based on dynamic sliding mode controller (DSMC) are proposed which is used to control Duffing-Holmes chaotic system (DHC). To solve the problem of DSMC, neural observer is used. Two neural observers are presented, the first observer is based on accessible system states and the observer error converges to a bound which is not guaranteed to be small, but in the second neural observer we only use system output and we prove observer error converges to zero. Because of using DSMC, chattering is removed completely. Moreover, the proposed approach preserves all the main properties of SMC such as invariance and simplicity in the design and implementation. Simulation results show the effectiveness of these approaches.

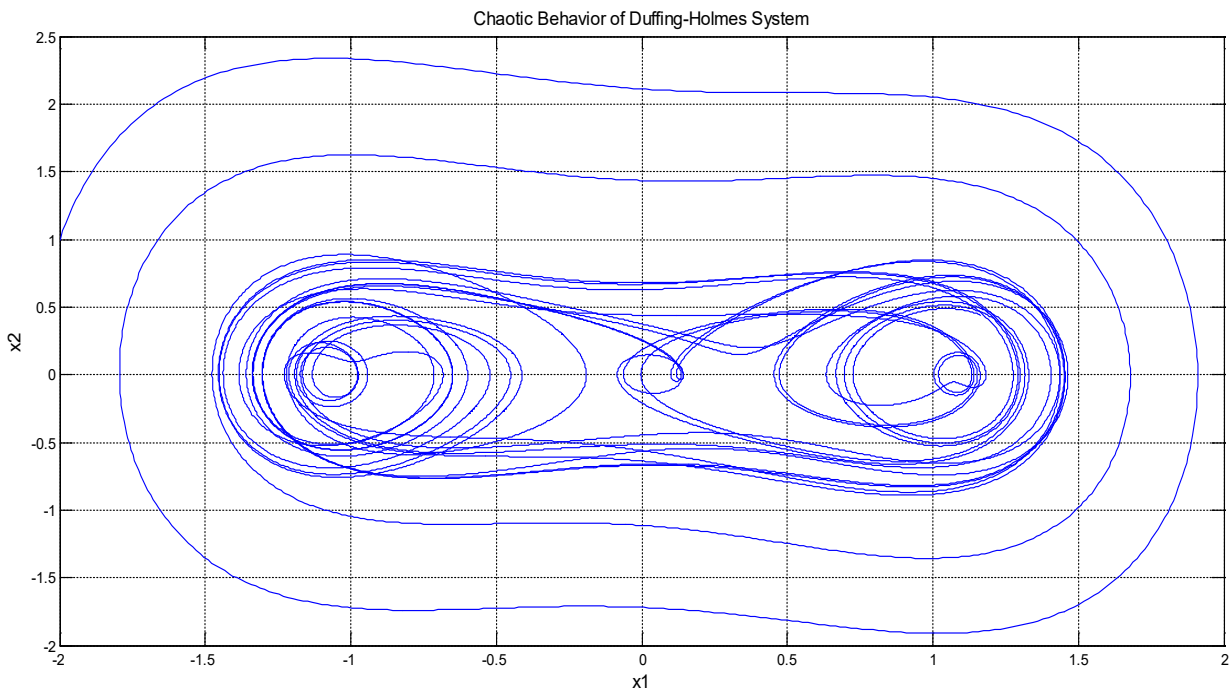


Fig. 1. Chaotic behavior of Duffing-Holmes system

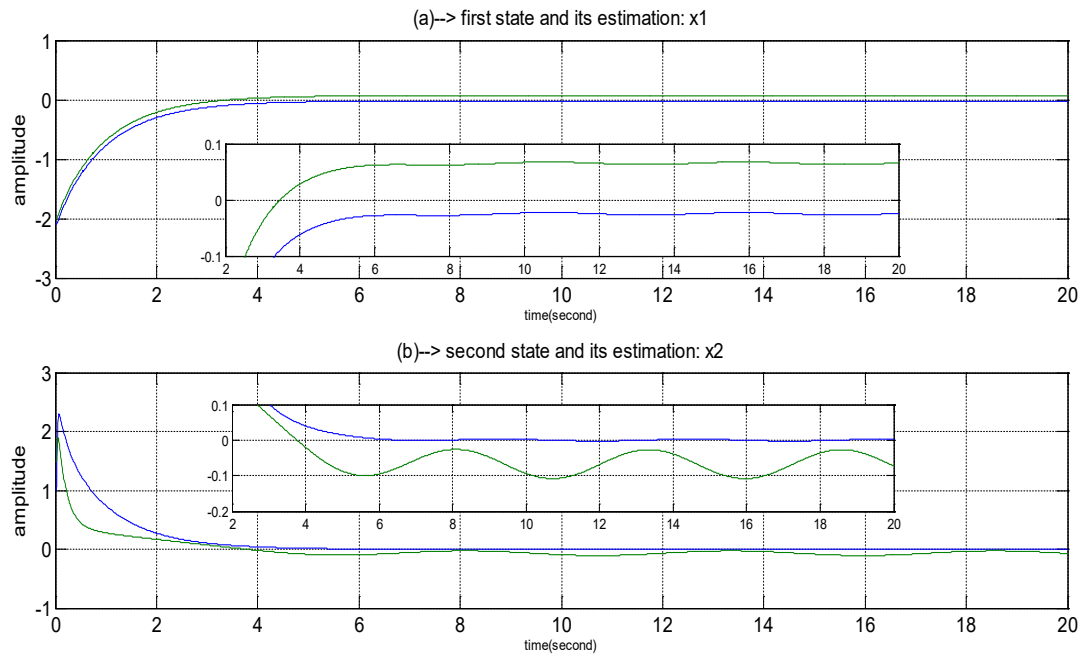


Fig. 2. System states and their estimations (a) first state and (b) second state (in example 1)

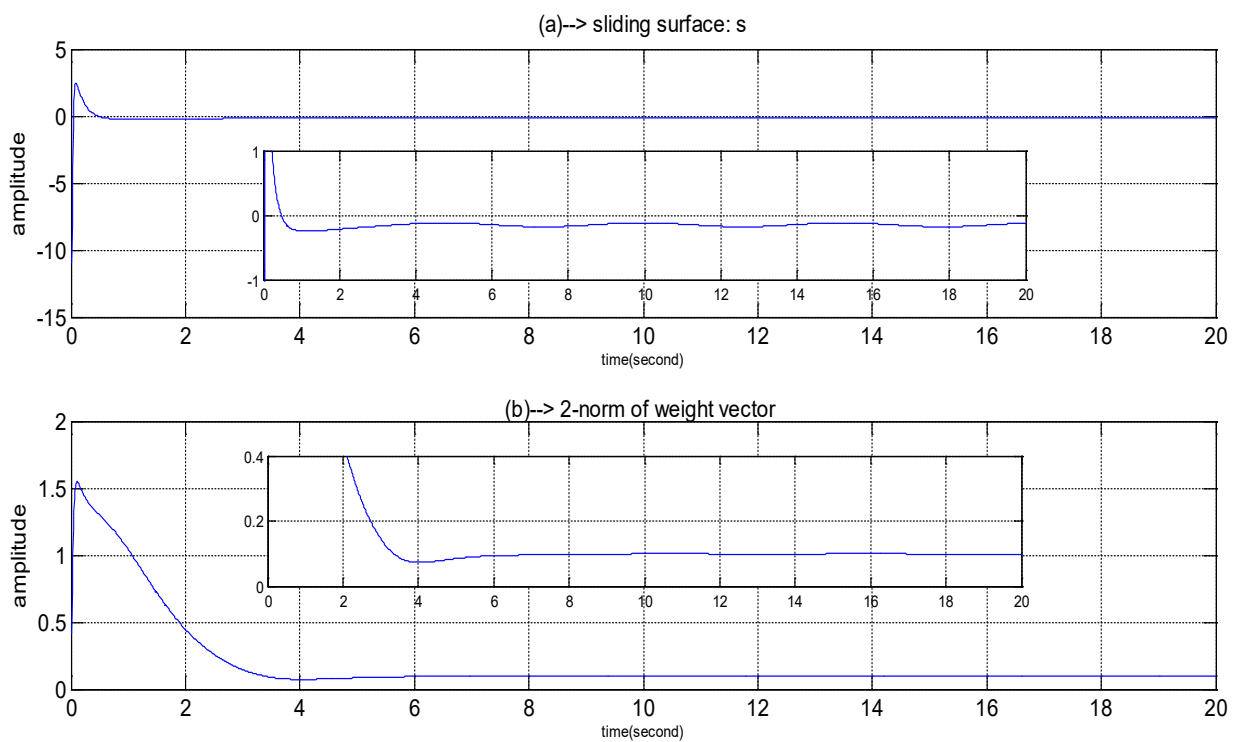


Fig. 3. (a) sliding surface and (b) norm of weights matrix (in example 1)

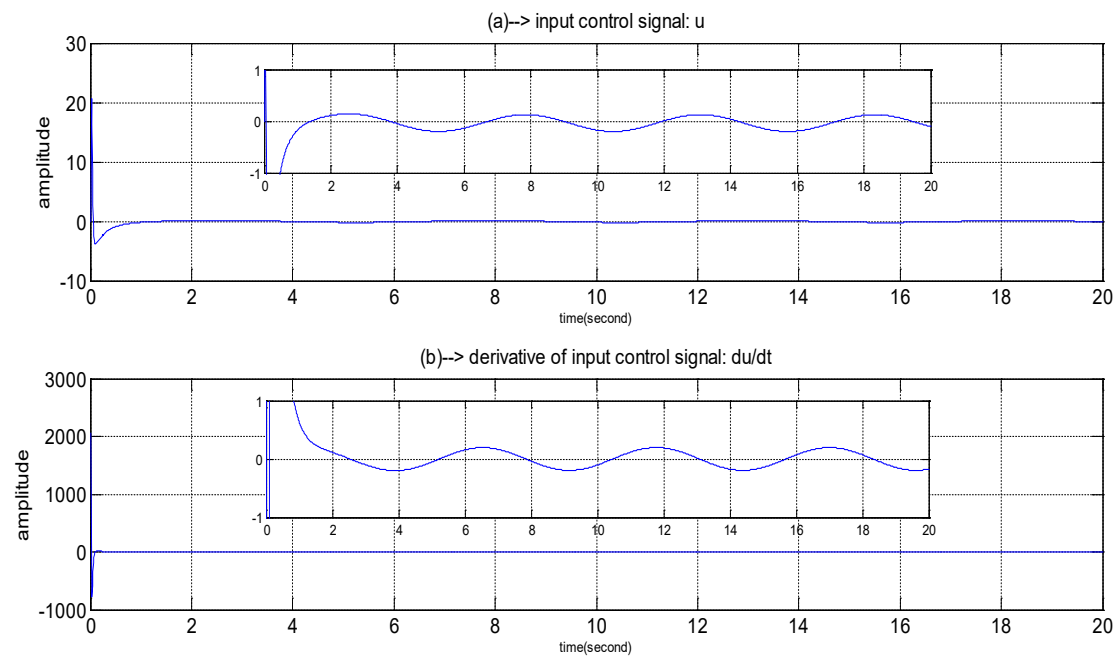


Fig. 4. (a) input control signal and (b) derivative of input control signal (in example 1)

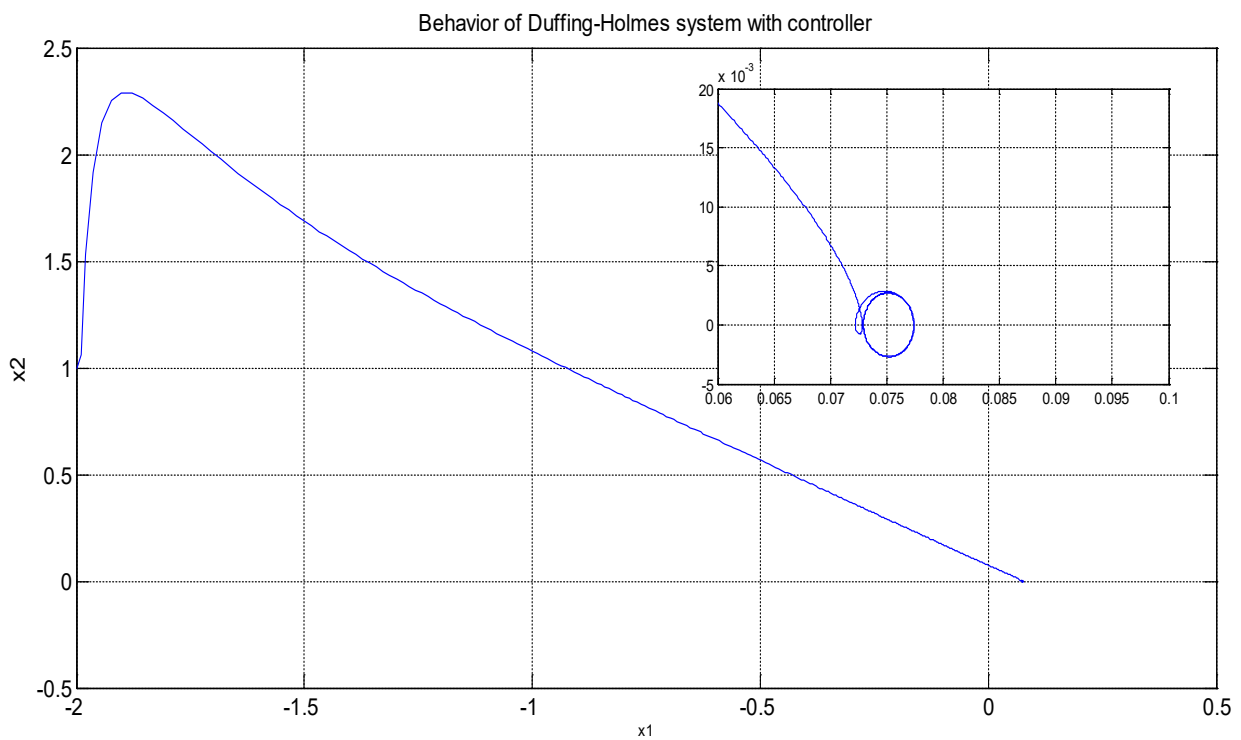


Fig. 5. Behavior of Duffing-Holmes system (in example 1)

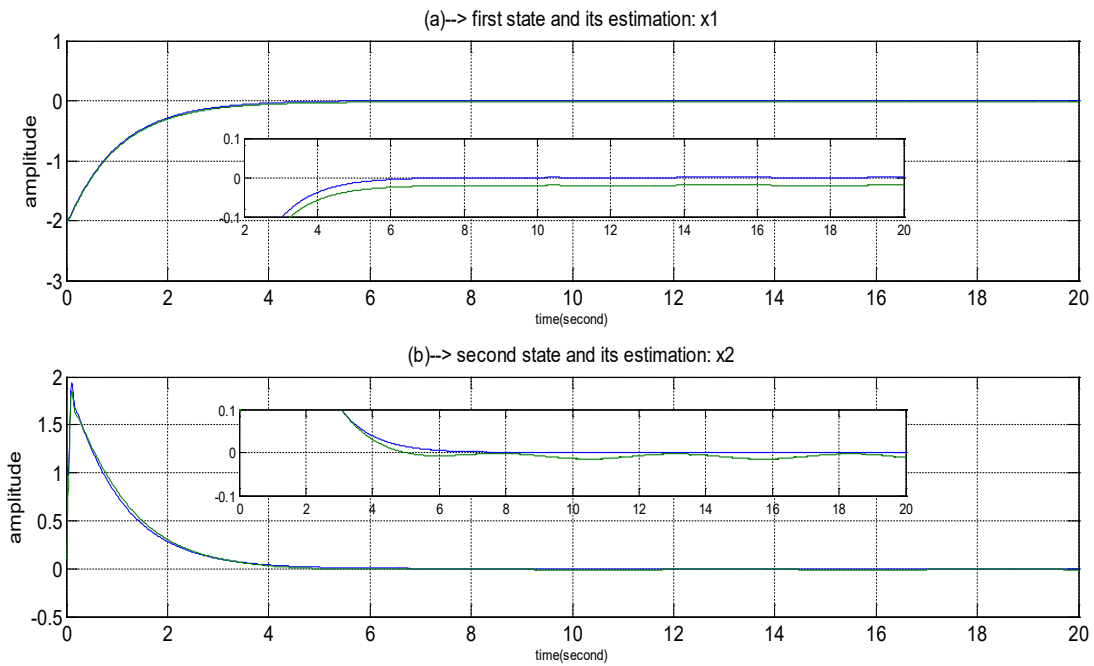


Fig. 6. System states and their estimates: (a) first state and (b) second state (in example 2)

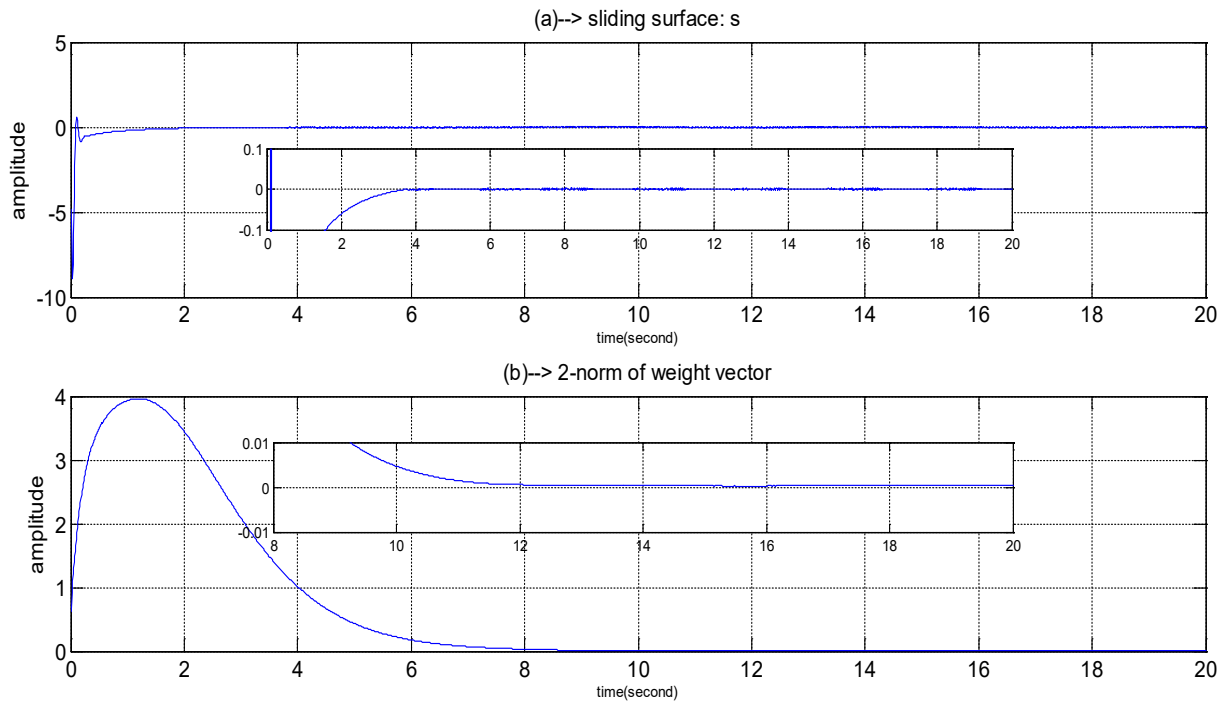


Fig. 7. (a) sliding surface and (b) norm of weights matrix (in example 2)

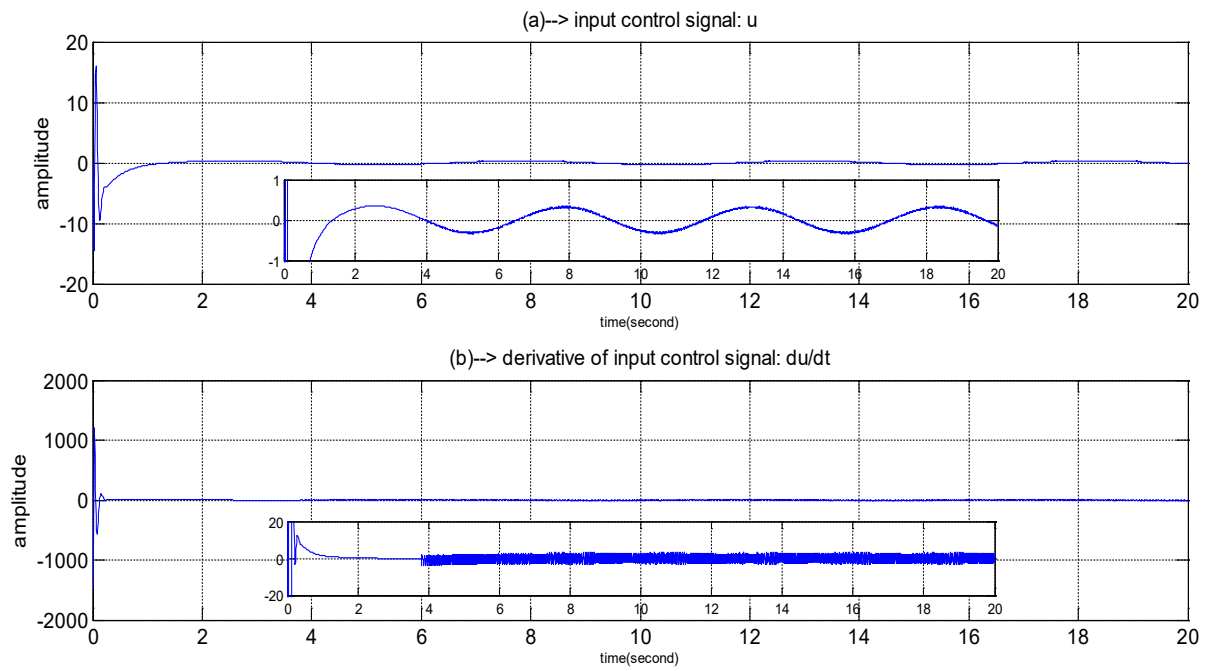


Fig. 8. (a) input control signal and (b) derivative of input control signal (in example 2)

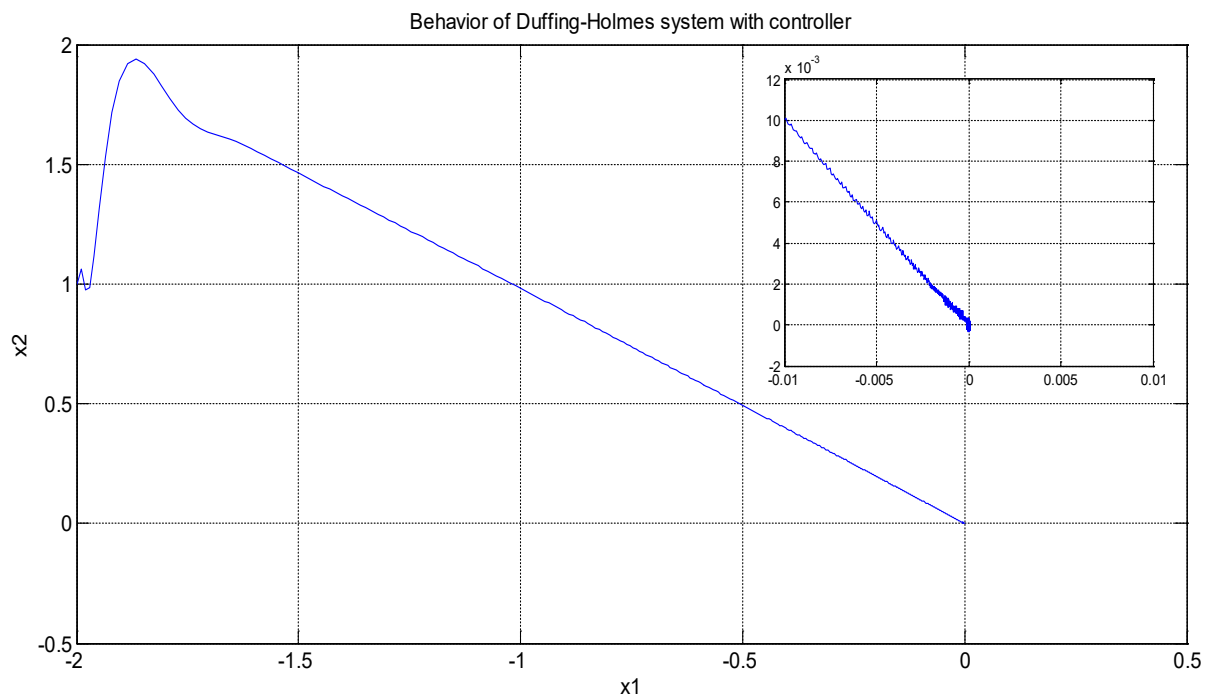


Fig. 9. Behavior of Duffing-Holmes system (in example 2)

References

- [1] J.-J. E. Slotine, W. Li, *Applied nonlinear control*, Prentice-Hall, 1991.
- [2] H. Lee, V.-I. Utkin, *Chattering suppression methods in sliding mode control systems*, Elsevier, *Annual Review in Control*, 31 (2007) 179-188.
- [3] A. Karami-Mollaei, N. Pariz, H. M. Shanechi, Position control of servomotors using neural dynamic sliding mode, *Transactions of the ASME (American Society of Mechanical Engineering), Journal of Dynamic Systems, Measurement and Control*, 133 (6) (2011) 141-150.
- [4] W. Perruquetti, J. Pierre-Barbot, *Sliding mode control in engineering*, Marcel Dekker, 2002.
- [5] T. Sun, H. Pei, Y. Pan, H. Zhou, C. Zhang, Neural network-based sliding mode adaptive control for robot manipulators, Elsevier, *Neurocomputing*, 74(14-15) (2011) 2377-2384.
- [6] M.-J. Zhang, Z.-Z. Chu, Adaptive sliding mode control based on local recurrent neural networks for underwater robot, Elsevier, *Ocean Engineering*, 45 (2012) 56-62.
- [7] Y. Zou, X. Lei, A compound control method based on the adaptive neural network and sliding mode control for inertial stable platform, Elsevier, *Neurocomputing*, 155 (2015) 286-294.
- [8] S. Mefoued, A second order sliding mode control and a neural network to drive a knee joint actuated orthosis, Elsevier, *Neurocomputing*, 155 (2015) 71-79.
- [9] H. M. Kim, S. H. Park, S. I. Han, Precise friction control for the nonlinear friction system using the friction state observer and sliding mode control with recurrent fuzzy neural networks, Elsevier, *Mechatronics*, 19 (2009) 805-815.
- [10] A. Levant, Sliding order and sliding accuracy in sliding mode control, *International Journal of Control*, 58 (1993) 1247-1263.
- [11] G. Bartolini, A. Ferrara, E. Usai, Chattering avoidance by second-order sliding mode control, *IEEE Transaction on Automatic Control*, 43(2) (1998) 241-246.
- [12] A. Levant, Robust exact differentiation via sliding mode techniques, Elsevier, *Automatica*, 34 (1998) 379-384.
- [13] M. Norgaard, O. Ravn, N. K. Poulsen, L. K. Hansen, *Neural network for modeling and control of dynamic systems*, Springer, New York, 2001.
- [14] C.-H. Lin, Recurrent wavelet neural network control of a PMSG system based on a PMSM wind turbine emulator, *Turkish Journal of Electrical Engineering & Computer Sciences*, 22(4) (2014) 795-824.
- [15] O. Kaynak, K. Erbatır, R. Ertugrul, The fusion of computationally Intelligent methodologies and sliding-mode control- a survey, *IEEE Transaction on Industrial Electronic*, 48(1) (2001) 4-17.
- [16] M. K. Sifakis, S. J. Elliott, Strategies for the control of chaos in a Duffing-Holmes oscillator, Elsevier, *Mechanical Systems and Signal Processing*, 14(6) (2000) 987-1002.
- [17] M. K. Sifakis, S. J. Elliott, Adaptive tracking control of Duffing-Holmes chaotic systems with uncertainty, *The 5th International Conference on Computer Science & Education*, Hefei, China, August 24-27, 2010, pp. 1193-1197.

Please cite this article using:

A. Karami-Mollaei and H. Shanechi, Dynamic Sliding Mode Control of Nonlinear Systems Using Neural Networks, *AUT J. Model. Simul. Eng.*, 50(1)(2018) 51-60.
DOI: 10.22060/miscj.2017.12805.5043

